

Effect of the pseudogap on the Hall conductivity in underdoped $\text{YBa}_2\text{Cu}_3\text{O}_{6+x}$.

Z.A. Xu*, Y. Zhang and N. P. Ong

Joseph Henry Laboratories of Physics, Princeton University, Princeton, New Jersey 08544

(February 5, 2020)

In underdoped $\text{YBa}_2\text{Cu}_3\text{O}_x$ (YBCO) with $x = 6.63$, the opening of the pseudogap at $T_s \simeq 160\text{K}$ has a strong effect on the Hall angle $\tan\theta$. While the Hall response is significantly reduced, the diagonal current is relatively unaffected. We present evidence that the Hall suppression continues below T_c down to 40 K. In the flux-flow state the Hall conductivity is also qualitatively different from that in optimally doped YBCO.

72.15.Gd,74.72.Bk,74.25.Fy,74.40.+k

In the underdoped cuprates, there is now strong evidence that a pseudogap gradually develops at temperatures significantly above the superconducting transition temperature T_c . Early evidence for a spin-gap in $\text{YBa}_2\text{Cu}_3\text{O}_x$ (YBCO) was obtained from the nuclear magnetic resonance (NMR) relaxation rate of the in-plane Cu ions Cu(2) [1–3]. Recently, angle-resolved photoemission experiments [4,5] have provided detailed confirmation of pseudogap formation in underdoped $\text{Bi}_2\text{Sr}_2\text{CaCu}_2\text{O}_{8+x}$. These experiments reveal a pseudogap with a \mathbf{k} -dependence consistent with that of the d -wave superconducting order parameter. The nature of the pseudogap phase is a subject of strong current interest [6–9]. Some of the key issues include the nature of electron pairing that leads to the formation of the pseudogap, and the possibility of experimentally distinguishing the effects of the pseudogap state on the charge and spin degrees of freedom.

Electrical transport is an important probe for investigating the effect of the pseudogap on the charge degrees of freedom. In underdoped $\text{YBa}_2\text{Cu}_3\text{O}_x$ with $x \simeq 6.63$, the in-plane resistivity ρ displays a distinct deviation from T -linear dependence that has been associated with the onset of the pseudogap [10]. However, from the NMR relaxation rate the spin-gap formation temperature T_s is estimated [2,3] to fall between 150 and 170 K in $\text{YBa}_2\text{Cu}_3\text{O}_{6.63}$, which is much lower than the temperature at which curvature in ρ first appears (250 K). Moreover, the appearance of a gap structure with strong \mathbf{k} dependence should affect the Hall effect, which is sensitive to the local Fermi Surface curvature. However, the Hall coefficient R_H in underdoped YBCO is quite featureless at 250 K. Instead, it peaks at a much lower temperature (120 K). Motivated by the strong interest in these issues, we have re-examined with improved resolution both the Hall effect and magnetoresistance (MR) in 60-K YBCO.

Our results show that pseudogap formation at T_s strongly affects the Hall angle, but leaves the resistivity relatively unperturbed. This remarkable selectivity accounts for the distinct profile of R_H . We also show that these effects extend deep into superconducting state where the Hall conductivity displays behavior very different from that in optimally-doped YBCO.

Twinned crystals of YBCO were sealed in a quartz tube with prepared polycrystalline $\text{YBa}_2\text{Cu}_3\text{O}_x$ with $x \simeq 6.63$ and annealed at 500 C for 2 weeks, before quenching in liquid nitrogen ($T_c = 61.0$ and 62.5.0 K in samples 1 and 2, respectively). At each T , we measured both $\rho_{xx} = \rho$ and $\rho_{xy} \equiv \rho_H$ versus a field $\mathbf{H} \parallel \mathbf{c}$ (with current density \mathbf{J} in-plane), and computed the Hall conductivity σ_H as well as the Hall angle $\theta = \arctan(\rho_H/\rho)$.

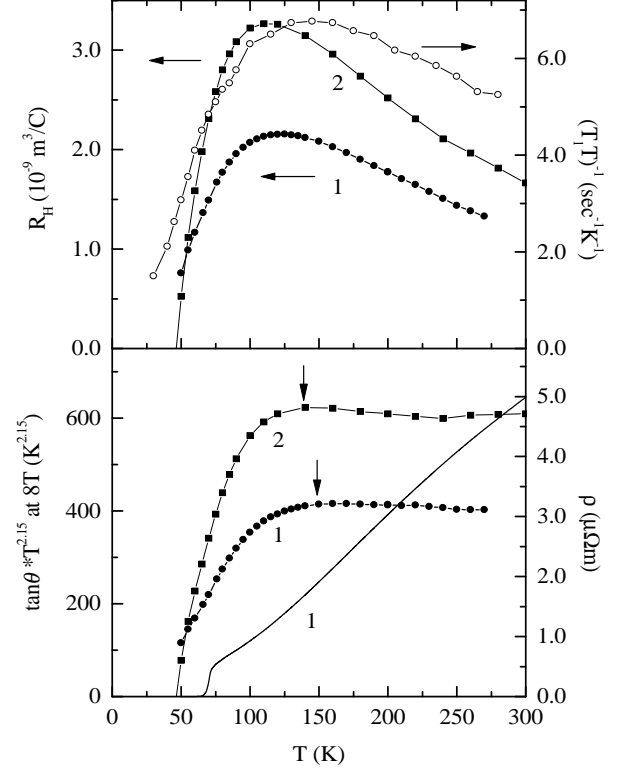


FIG. 1. (Upper Panel) The temperature dependence of the in-plane Hall coefficient $R_H = \rho_H/B$ (solid symbols) in 2 crystals of twinned underdoped $\text{YBa}_2\text{Cu}_3\text{O}_{6.63}$ measured with $\mathbf{H} \parallel \mathbf{c}$. In both crystals, R_H attains a maximum at 115 K. The open symbols are the Cu(2) NMR relaxation rate $(T_1 T)^{-1}$ measured by Takigawa et al. in YBCO ($x = 6.63$). The lower panel shows ρ at $H = 0$ (sample 1) and the Hall angle θ in the two crystals plotted as $T^\eta \tan\theta$ with $\eta = 2.15$. Deviation of $\tan\theta$ from its high-temperature power law starts near 150 K (arrows).

In the limit ρ_{xx} and $\rho_H \rightarrow 0$ ($B \rightarrow 0$) (the regime of interest here), σ_H is sensitive to alignment problems, especially near the critical temperature T_c . We have adopted the following procedure to address this specific problem. At each T , the field is swept from -8 T to 8 T (in 20 min.), followed by a sweep back to 8 T (the double sweeps are necessary to correct for the misalignment problems). To stabilize T to the level of ± 5 mK (as indicated by the retracing of ρ in the four sweeps), we pre-amplified the thermometer signal before feeding it to the regulator. The measurements are then repeated at a slower sweep rate over the interval ± 1 T to improve the resolution in weak fields. Hall curves obtained from 3 crystals are closely similar.

The Hall coefficient R_H (Fig. 1, upper panel) displays a broad peak at 120 K, followed by a steep decrease as $T \rightarrow T_c$, in good agreement with previous work [12,10]. It is also known that the Cu(2) NMR relaxation rate plotted as $(T_1 T)^{-1}$ goes through a broad peak at a slightly higher temperature (we show the data of Takigawa et al. for YBCO with $x = 6.63$ [3]). The close proximity of the maxima in R_H and $(T_1 T)^{-1}$ suggests that the two measurements may be closely related. Instead of R_H , however, it is preferable to examine the Hall angle, which provides a cleaner indicator of the Hall response.

In the lower panel (Fig. 1), we have plotted the resistivity ρ and the Hall angle as $T^\eta \tan \theta$ to factor out the high-temperature dependence (the exponent $\eta = 2.15$ is slightly larger than the value 2.0 in 93-K YBCO [11]). The plots show that $\tan \theta$ follows the power law $1/T^\eta$ closely until 155 ± 5 K where it starts deviating downwards. This temperature is quite close to the value of T_s (160 K) inferred from the NMR relaxation rate. By contrast, ρ starts deviating from its T -linear behavior at the higher temperature 250 K (we note that $T^\eta \tan \theta$ is quite flat across this temperature.)

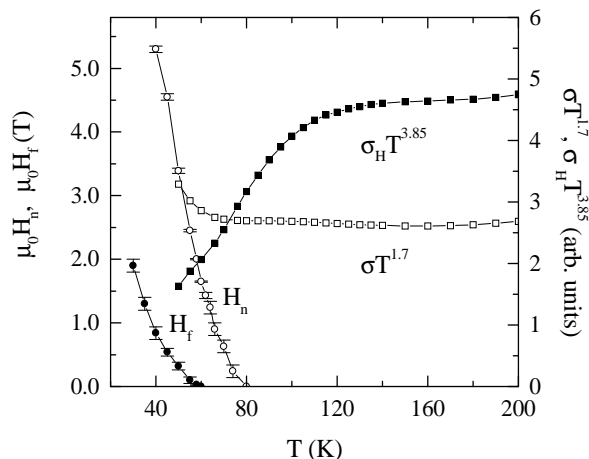


FIG. 2. Plots of the conductivities σ_H (solid squares) and σ (open squares), with their high- T power law factored out (sample 1). The selective effect of the pseudogap on σ_H is apparent below 150 K. Also shown are the field scales H_n (open circles) and H_f (closed circles).

It is instructive to examine the behavior of the conductivity $\sigma \equiv 1/\rho$ and the (weak-field) Hall conductivity $\sigma_H = \tan \theta / \rho$. At high T , σ_H displays the power-law dependence $T^{-3.85}$. Factoring out this power-law, we compare it with σ in Fig. 2. Whereas σ_H exhibits the same downturn below 155 K as the Hall angle, the T -dependence of σ itself remains unperturbed. These comparisons reveal that pseudogap formation affects selectively the Hall channel; they appear to have little effect on the diagonal conductivity. The selectivity again emphasizes the distinctive scattering processes that affect $\tan \theta$ and ρ differently. Previously, the anomalous T dependence of R_H in optimally-doped YBCO was shown to derive from distinct power-laws in $\tan \theta$ and ρ [11]. Here, we find that the pseudogap in underdoped YBCO selectively affects the former but not the latter.

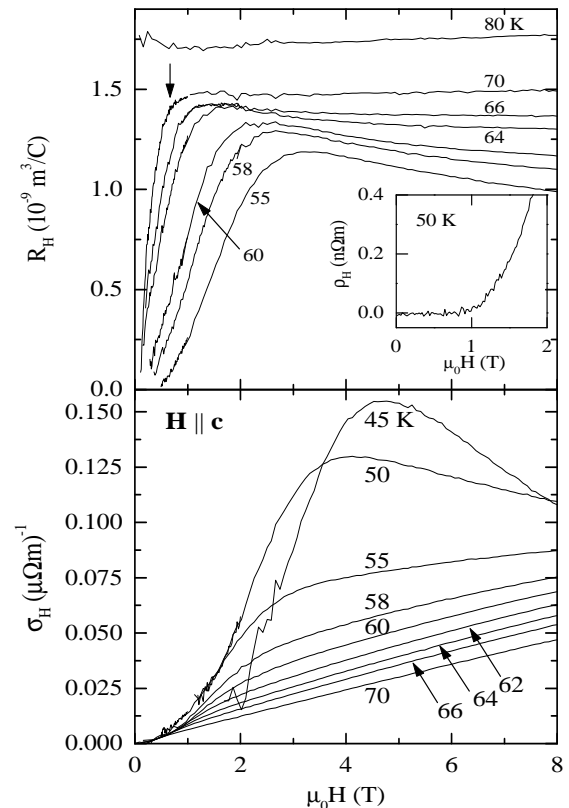


FIG. 3. (Upper Panel) The field dependence of R_H at selected T (sample 1). Below 80 K, R_H displays an anomalous decrease to zero in weak fields. The structure of this Hall anomaly evolves smoothly through the transition temperature T_c . The inset shows ρ_H at 50 K at high resolution. The negative ‘dip’ that characterizes ρ_H in the flux-flow state in 93-K crystals is absent. The lower panel shows the field dependence of the Hall conductivity $\sigma_H = \rho_H / (\rho_{xx}^2 + \rho_H^2)$ in sample 1. Below ~ 64 K, the weak-field anomaly appears as a prominent ‘missing area’ in the field profile. In the limit $H \rightarrow 0$, $\sigma_H \sim H^2$.

This selectivity also accounts for the characteristic profile of R_H in underdoped YBCO. The steep decrease in σ_H , together with an unchanged σ (in relative terms),

produces a broad peak in R_H at 120 K, followed by a rapid decrease at lower T . (We also note that the peak moves to higher T as x decreases consistent with a pseudogap effect [10]). Previously, the steep decrease in R_H below 120 K was mis-identified as the conventional Hall contribution from superconducting fluctuations [8]. The present evidence suggests that it is rather caused by the selective influence of the pseudogap on the Hall current. Fluctuations associated with superconductivity appear (with their own characteristics) only at a much lower T (80 K).

To substantiate this view, we next examine the transport behavior in both the fluctuation and flux-flow regimes. The transport features in these regimes are quite distinct from those in 93-K YBCO. In particular, we observe an anomaly in σ_H that suggests a close relation between the Hall current below T_c and in the pseudogap phase.

The upper panel of Fig. 3 shows the field dependence of R_H at selected T . At and above 80 K, R_H is *independent* of field, within our resolution. Below 80 K, however, a weak-field anomaly becomes apparent as a rapid decrease in R_H to zero in the limit $H \rightarrow 0$. At temperatures above T_c , the steep variation of R_H in weak fields terminates quite abruptly at a characteristic field H_n above which R_H is H -independent. At 70 K, for e.g., we estimate $H_n \simeq 0.6$ T (arrow) (H_n is plotted vs. T in Fig. 2). The Hall anomaly becomes quite striking below T_c . In the lower panel, we have plotted the field dependence of σ_H . While the anomaly is barely resolved in weak fields at 70 K, it grows to a prominent ‘missing area’ in the field profile below 60 K. Both above and below T_c , σ_H has the limiting form $\text{sgn}(H)H^n$ (as $H \rightarrow 0$), with an anomalous exponent $n = 2 \pm 0.2$.

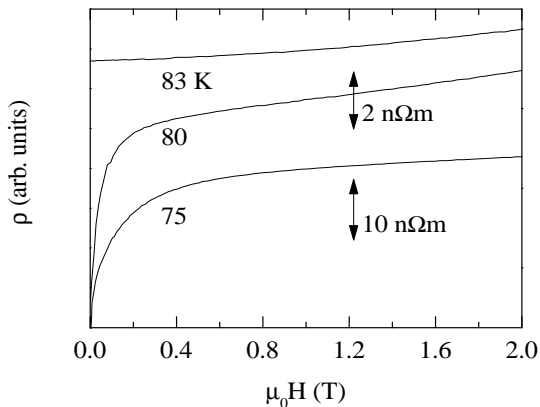


FIG. 4. The magnetoresistance in sample 1 near 80 K shown at high resolution (sample 1). The vertical scales are indicated by the double arrows.

The rather abrupt appearance of the Hall anomaly at 80 K is matched by the appearance of a weak-field anomaly in the MR (Fig. 4). At and above 83 K, ρ displays only the weak H^2 MR associated with the normal state. Below 83 K, however, a weak-field cusp is observed.

It is worth a remark that the cusp (and the weak-field Hall anomaly) represent the first *field-sensitive* transport features that become observable as T is lowered from 300 K. Below T_c , the cusp magnitude increases rapidly as the resistivity evolves into the usual flux-flow profile. The onset of dissipation in the resistive state is marked by a fairly well-defined threshold field H_f (the curve for H_f is displayed in Fig. 2).

Both the Hall anomaly and the cusp in the MR are clearly associated with the field suppression of superconducting droplets as we approach T_c . However, we emphasize that these two features are poorly described by the standard fluctuation conductivity calculations based on Aslamasov-Larkin (AL) theory. Whereas the AL theory explains reasonably well the fluctuating conductivity measured in 93-K crystals, the field dependence of ρ here is far too large and rapid to be described by these perturbation results. The fairly abrupt appearance of the weak-field cusp at 80 K is quite different from the power-law dependence (on reduced temperature ϵ) of the AL fluctuation terms [13].

At temperatures above T_c , σ_H is also inconsistent with the conventional fluctuation picture. The weak-field exponent n is incompatible with the fluctuation Hall conductivity calculated, for e.g., from time-dependent Ginzburg Landau (GL) theory, which has the H -linear form [14,8] $\delta\sigma_H = (e^2/3\pi d)\gamma^n (T_c/g)eH\xi_0^2/\hbar c^2$, where ξ_0 is the GL coherence length, and γ^n and g are GL parameters.

More significantly, the Hall current in underdoped YBCO in its mixed state above 40 K is strikingly different from that in 93-K YBCO (over the same range in reduced T). It is well known that, in 93-K YBCO, the flux-flow Hall resistivity exhibits a sign change that appears abruptly below T_c as a prominent negative ‘dip’ in the profile of ρ_H vs. H [11,15,16]. The non-monotonic ρ_H simplifies considerably when converted to σ_H [15,16]; the latter is simply the sum of a positive quasiparticle (qp) term σ_H^{qp} and a negative vortex-flow term σ_H^f , viz. $\sigma_H = \sigma_H^{qp} + \sigma_H^f$, with H dependences

$$\sigma_H^{qp} \sim H, \quad \sigma_H^f \sim -1/H. \quad (1)$$

The $1/H$ divergence in σ_H^f is a firm prediction of many theories [17]. Experimentally, it shows up in 93-K YBCO as the characteristic negative ‘dip’ in ρ_H .

By contrast, ρ_H in 60-K YBCO shows no evidence of the negative ‘dip’ feature above 40 K. At 50 K, for instance, the onset of dissipation (ρ) occurs abruptly at 0.35 T. However, the Hall resistivity ρ_H is unresolved from zero until about 0.8 T, above which it increases in the *positive* direction (inset in lower panel of Fig. 2). The absence of the $1/H$ divergence in σ_H is also apparent in the traces in the lower panel of Fig. 3. Other aspects of σ_H are also different from that in Eq. 1. Instead of increasing monotonically, σ_H is nominally H^2 at low fields and attains a broad maximum at high fields. Thus, between 40 and 60 K, the vortex Hall conductivity term σ_H^f

is conspicuously absent. This is possibly the most striking difference observed so far in vortex transport properties between underdoped and optimally-doped YBCO. It implies that, in the former above 40 K, the vortices move very nearly parallel to $\mathbf{J} \times \mathbf{H}$, i.e. the flux-flow electric field contributes only to ρ_{xx} . (Only below 30 K does the vortex Hall contribution become apparent [18]. Below 20 K, the vortex Hall angle rapidly approaches the superclean regime.)

The absence of σ_H^f at the temperatures where the Hall anomaly is most prominent persuades us that the latter reflects changes to the electronic state, as reflected in σ_H^{qp} . We note that, on both sides of T_c (Fig. 3), σ_H exhibits the same anomalous H^2 dependence in low fields. In our view, the continuous behavior of the Hall anomaly across T_c implies that it represents the same feature in the electronic current on both sides of T_c . The traces in Fig. 3 imply that the increased phase coherence near T_c leads to an electronic state (below the line H_n) in which the Hall conductivity is severely suppressed. The similarity of this suppression to the Hall-angle suppression at 155 K is highly suggestive. The high-temperature suppression appears to be a less complete precursor of the more complete suppression that occurs below 80 K (but it is more robust in field).

In conclusion, we find that the pseudogap onset temperature T_s , as derived from NMR, correlates more closely with the downturn in $\tan\theta$, rather than with ρ . Below T_s , both $\tan\theta$ and σ_H are suppressed significantly, whereas σ is relatively unaffected. Within the broad interval 80 to 160 K, in which the selective effect of the pseudogap on the two currents is fully apparent, the effects of superconducting fluctuations are either non-existent or too small to be resolved by transport experiments. Fluctuations (insofar as they are field sensitive) become apparent only below 80 K, where the Hall anomaly and the cusp in the MR first appear. At the high temperature side, the fluctuation regime is clearly demarcated by the field H_n . The rapid growth of phase coherence produces a weak-field anomaly in σ_H that corresponds to a further suppression of the Hall conductivity. In the mixed state, our measurements show that the contribution of the vortices to the Hall current is unobservable above 40 K. This implies that the suppression of σ_H is associated with the quasiparticle current. Unlike in 93-K crystals, the pseudogap state displays a rather rich array of transport features that evolve between 160 K and 40 K. These results seem to provide a more complete picture of the effect of the pseudogap on the transport properties in underdoped YBCO than previously available.

We gratefully acknowledge many helpful discussions with P.W. Anderson, P. A. Lee, A. Millis, S. Uchida and X. G. Wen. The research is supported by the National Science Foundation (MRSEC grant DMR98-09483), and by an International Joint-Research Grant from the New Energy and Industrial Tech. Devlop. Org. (NEDO) of

Japan.

**Permanent address:* Department of Physics, Zhejiang University, Hangzhou 310027, China

-
- [1] T. M. Rice in *The Physics and Chemistry of Oxide Superconductors*, ed.s. Y. Iye and H. Yasuoka (Springer Verlag, 1992), p. 313.
 - [2] H. Yasuoka *et al.* in *Strong Correlation and Superconductivity*, eds. H. Fukuyama, S. Maekawa and A. P. Malozemoff (Springer Verlag, 1989), p. 254; R. E. Walstedt *et al.*, Phys. Rev. B **41**, 9574 (1990); H. Alloul *et al.*, Phys. Rev. Lett. **67**, 3140 (1991).
 - [3] M. Takigawa, A. P. Reyes, P. C. Hammel, J. D. Thompson, R. H. Heffner, Z. Fisk, and K. C. Ott, Phys. Rev. B **43**, 247 (1991).
 - [4] J. M. Harris, Z.-X. Shen, P. J. White, D. S. Marshall, M. C. Schabel, J. N. Eckstein, and I. Bozovic, Phys. Rev. B **54**, R 15665 (1996).
 - [5] H. Ding, T. Yokoya, J. C. Campuzano, T. Takahashi, M. Randeria, M. R. Norman, T. Mochiku, K. Kadowaki, and J. Giapintzakis, Nature **382**, 51 (1996).
 - [6] V. J. Emery and S. A. Kivelson, Nature **374**, 434 (1995).
 - [7] Patrick A. Lee and Xiao-Gang Wen, Phys. Rev. Lett. **78**, 4111 (1997).
 - [8] V. B. Geshkenbein, L. B. Ioffe, A. I. Larkin, Phys. Rev. B **55**, 3173 (1997).
 - [9] L. B. Ioffe and A. J. Millis, preprint (cond-matt/9801092).
 - [10] T. Ito, K. Takenaka, and S. Uchida, Phys. Rev. Lett. **70**, 3995 (1993).
 - [11] T. R. Chien, Z. Z. Wang, and N. P. Ong, Phys. Rev. Lett. **67**, 2088 (1991).; P. W. Anderson, *ibid.* **67**, 2084 (1991).
 - [12] J.M. Harris, Y.F. Yan, and N.P. Ong, Phys. Rev. B **46**, 14293 (1992).
 - [13] The analysis of the MR will be reported elsewhere. Z. A. Xu and N. P. Ong *in preparation*.
 - [14] A. G. Aronov, S. Hikami, and A. I. Larkin, Phys. Rev. B **51**, 3880 (1995); S. Ullah and A. T. Dorsey, Phys. Rev. B **44**, 262 (1991).
 - [15] J. M. Harris, N. P. Ong, P. Matl, R. Gagnon, L. Taillefer, T. Kimura and K. Kitazawa, Phys. Rev. B **51**, 12053 (1995).
 - [16] A. V. Samoilov, Z. G. Ivanov, and L.-G. Johansson, Phys. Rev. B **49**, 3667 (1994).
 - [17] P. Nozieres and W. F. Vinen, Philos. Mag. **14**, 667 (1966); N. B. Kopnin, B. I. Ivlev, and V. A. Kalatsky, J. Low Temp. Phys. **90**, 1 (1993); Alan T. Dorsey, Phys. Rev. B **46**, 8376 (1992).
 - [18] J.M. Harris, Y.F. Yan, O.K.C. Tsui, Y. Matsuda and N.P. Ong, Phys. Rev. Lett. **73**, 1711 (1994).